Since January 2020 Elsevier has created a COVID-19 resource centre with free information in English and Mandarin on the novel coronavirus COVID-19. The COVID-19 resource centre is hosted on Elsevier Connect, the company's public news and information website.

doi:10.1016/j.jmb.2006.07.050 J. Mol. Biol. (2006) 362, 539–554

JMB

Available online at www.sciencedirect.com

ScienceDirect

ELSEVIER

Histidine Triad-like Motif of the Rotavirus NSP2 Octamer Mediates both RTPase and NTPase Activities

Rodrigo Vasquez-Del Carpio[1], Fernando D. Gonzalez-Nilo[2] Gonzalo Riadi[2], Zenobia F. Taraporewala[1] and John T. Patton[1]*

[1]*Laboratory of Infectious Diseases, NIAID, National Institutes of Health, Bethesda MD 20892, USA*

[2]*Centro de Bioinformatica y Simulacion Molecular (CBSM) Universidad de Talca, 2 Norte 685, Casilla 721, Talca - Chile*

**Corresponding author*

Rotavirus NSP2 is an abundant non-structural RNA-binding protein essential for forming the viral factories that support replication of the double-stranded RNA genome. NSP2 exists as stable doughnut-shaped octamers within the infected cell, representing the tail-to-tail interaction of two tetramers. Extending diagonally across the surface of each octamer are four highly basic grooves that function as binding sites for single-stranded RNA. Between the N and C-terminal domains of each monomer is a deep electropositive cleft containing a catalytic site that hydrolyzes the γ-β phosphoanhydride bond of any NTP. The catalytic site has similarity to those of the histidine triad (HIT) family of nucleotide-binding proteins. Due to the close proximity of the grooves and clefts, we investigated the possibility that the RNA-binding activity of the groove promoted the insertion of the 5′-triphosphate moiety of the RNA into the cleft, and the subsequent hydrolysis of its γ-β phosphoanhydride bond. Our results show that NSP2 hydrolyzes the γP from RNAs and NTPs through Mg^{2+}-dependent activities that proceed with similar reaction velocities, that require the catalytic His225 residue, and that produce a phosphorylated intermediate. Competition assays indicate that although both substrates enter the active site, RNA is the preferred substrate due to its higher affinity for the octamer. The RNA triphosphatase (RTPase) activity of NSP2 may account for the absence of the 5′-terminal γP on the (−) strands of the double-stranded RNA genome segments. This is the first report of a HIT-like protein with a multifunctional catalytic site, capable of accommodating both NTPs and RNAs during γP hydrolysis.

Published by Elsevier Ltd.

Keywords: rotavirus replication; viroplasm formation; NSP2; RTPase activity; NTPase activity

Introduction

Rotaviruses, members of the *Reoviridae* family, are the leading cause of acute gastroenteritis in young children throughout the world.[1] The rotavirus virion is a triple-layered icosahedral particle containing 11 segments of double-stranded (ds)RNA.[2,3] Loss of the outer-most layer during entry give rises to a transcriptionally active double-layered particle (DLP) that directs the synthesis of viral (+)-strand RNAs.[4] The (+)-strand RNAs are replicated to dsRNAs and packaged into pre-virion core particles within large inclusion bodies (viroplasms) that form in the cytoplasm of the infected cell.[5–7] Interactions between two abundant non-structural proteins, NSP2 and NSP5, are essential for the formation of such inclusions.[8–10] These proteins are

Present address: R. Vasquez-Del Carpio, Structural Biology Program, Department of Molecular Physiology and Biophysics, Mount Sinai School of Medicine, New York, NY 10029, USA.

Abbreviations used: ds, double-stranded; ss, single-stranded; DLP, double-layered particle; RdRP, RNA-dependent RNA polymerase; NTPase, nucleoside-triphosphate phosphohydrolase; PKCI, protein kinase C-interacting protein; HIT, histidine triad; RTPase, RNA triphosphatase; VLS, viroplasm-like structure; TAP, tobacco acid pyrophosphatase.

E-mail address of the corresponding author: jpatton@niaid.nih.gov

0022-2836/$ - see front matter. Published by Elsevier Ltd.

also components of the replication intermediates that synthesize dsRNAs in viroplasms.[5,11,12] The association of NSP2 with such intermediates may be mediated by interaction with the viral RNA-dependent RNA polymerase (RdRP), VP1.[13]

NSP2 is a basic protein (M_r = 35,000) that self-assembles into stable doughnut-shaped octamers, formed by the tail-to-tail interaction of two tetramers (Figure 1).[14] The overall architecture of such octamers is highly conserved even among distantly related groups of rotaviruses.[15] The octamers possess single-stranded (ss)RNA-binding activity capable of destabilizing RNA–RNA duplexes by an ATP and Mg^{2+} independent mechanism.[16,17] In addition, the octamers have a Mg^{2+}-dependent nucleoside-triphosphate phosphohydrolase (NTPase) activity that cleaves the γ-β phosphoanhydride bond of any nucleoside triphosphate (NTP), yielding the products NDP and P_i.[16] Following cleavage, the γP is transferred to NSP2, generating a short-lived phosphorylated form of the protein.[16,18] The hydrolitic activity of NSP2 is essential for genome replication.[15] NSP2 octamers in the presence of NTPs undergo a conformational transition, shifting from a relaxed to a more condensed state as is typical of molecular motors.[19] Collectively, these properties have led to the suggestion that the NSP2 octamer may facilitate genome packaging and replication by relaxing secondary structures in viral template RNAs that impede polymerase function and by assisting in the translocation of viral RNAs into pre-virion cores.

The NSP2 monomer has two distinct domains (N and C-terminal), separated by an electropositive 25 Å deep cleft that contains residues involved in the binding and hydrolysis of NTPs. The location of the NTP-binding site was initially proposed based on the structural similarity of the C-terminal domain with the catalytic core of protein kinase C-interacting protein (PKCI), a prototypical member of the histidine triad (HIT) family of nucleotide-binding proteins.[14,20] Although lacking a precise signature HIT motif (HØHØHØØ, where is Ø is a hydrophobic residue), mutagenesis has indicated that conserved basic residues in the NSP2 cleft form a HIT-like motif (H^{221}-G-(K/H)-Ø-H^{225}-Ø-R-V) responsible for the binding and hydrolysis of NTPs.[18] More recently, data obtained by co-crystallization of NSP2 with nucleotide analogs has shown that His225 is the catalytic residue of the motif, becoming phosphorylated through the covalent attachment of the γP released during attack on the γ-β phosphoanhydride bond of the NTP.[21] In contrast, the catalytic histidine of HIT proteins traditionally undergoes nucleotidylation by way of an αP linkage formed during attack of the β–α phosphoanhydride bond of the nucleotide substrate.[20]

Extending diagonally across the NSP2 octamer surface are four highly basic grooves, 30 Å wide and 25 Å deep, that function as ssRNA-binding sites.[14,22] Each groove is lined by two 24-residue electropositive loops, originating between the two subdomains of the N terminus of each monomer (Figure 1). The location of these loops is such that they position the electropositive residues at the entrance of the catalytic clefts containing the HIT-like motif. Due to the close proximity of the grooves and clefts, binding of ssRNA in a groove may impact the passage of NTPs into or out of the cleft and, therefore, may influence the NTPase activity of the octamer. On the other hand, interaction of ssRNA with a groove may promote entry of the triphosphorylated 5′ end of the bound RNA into the cleft, an event that may be further advanced by the strongly electropositive characteristics of the cleft residues. Given that the interior dimensions of the cleft are sufficient to accommodate ssRNA,[14] we investigated the possibility that the NSP2 octamer could function as an RNA triphosphatase (RTPase), wherein those same residues involved in NTP

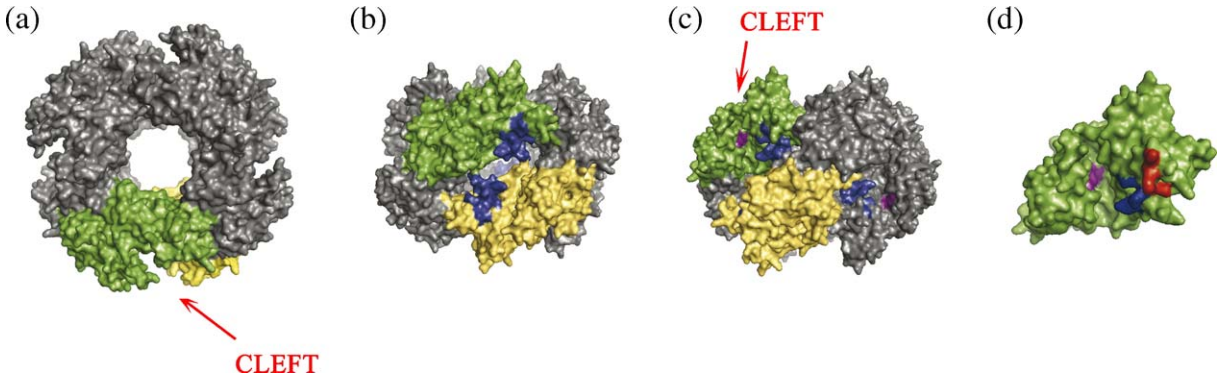

Figure 1. Structural proximity of the NTP-binding cleft and the RNA-binding grooves. Surface representation of the NSP2 octamer viewed along the 4-fold (a) and 2-fold axes ((b) and (c)). Two monomers have been identified in the octamer (green and yellow). The image in (b) represents a 90° rotation along the *x*-axis with respect to the image in (a). Residues 53 to 76 that form part of the electropositive loops, which line the RNA-binding grooves, are denoted in blue. (c) The image in (b) was rotated 45° clockwise along the *y*-axis to allow visualization into the cleft. Residues within the cleft that make up the active site for NTP hydrolysis are shown in purple. (d) Surface representation of one monomer as viewed in (c). The residues selected for glutamine mutagenesis are shown in red (K^{37}, K^{38}, K^{58}) and blue (K^{59}, R^{60}, R^{68}). Images were prepared using PyMOL [http//pymol.sourceforge.net/].

hydrolysis would direct the cleavage of the γ-β phosphoanhydride bond at the 5′ end of a ssRNA.

Herein, we show that the NSP2 octamer has RTPase activity, and that the RTPase and NTPase activities of the octamer utilize the same HIT-like motif and generate indistinguishable phosphorylated intermediates. Our analysis also indicates that ssRNA is preferred as a substrate over NTPs in hydrolysis reactions, likely due to the higher affinity of the octamer for ssRNA. Overall, the results suggest that ssRNAs represent a legitimate substrate for the hydrolytic activity of NSP2 during the rotavirus replication cycle. This activity may account for the absence of the γP at the 5′ end of the (−) strands that make up the rotavirus dsRNA genome. This is the first report of a protein using a HIT-like motif to direct RTPase activity.

Results

RTPase activity of NSP2

The HIT-like motif of the NSP2 monomer is contained in a cleft with dimensions adequate for entry of a ssRNA. To explore the possibility that this architecture would allow NSP2 to function as an RTPase (Figure 2(a)), we prepared [γ-^{32}P]5′g8 RNA, a probe representing the first 21 residues of the rotavirus gene *8* RNA radiolabeled only at the γP position (Figure 2(b)). The RNA was incubated with octamers of wild-type NSP2 (*wtNSP2*) and of an NSP2 mutant that lacks NTPase activity due to mutation of the catalytic H^{225} residue (*H225A*), under reaction conditions used earlier for NTPase assays.[18] As shown by thin-layer chromatography (TLC) of the reaction products (Figure 2(c)), *wtNSP2* but not *H225A*, catalyzed the hydrolysis of the γP from the ssRNA. Like the NTPase activity of NSP2, hydrolysis of the γP from RNA was dependent on Mg^{2+} in reaction mixtures (data not shown). These results are consistent with NSP2 functioning as an RTPase, potentially utilizing the same residues in the cleft needed for NTP hydrolysis (e.g. H^{225}).

The 5′ cap structure of rotavirus (+)-strand RNAs consists of an inverted methylated guanosine bridged to the 5′-terminal G (+1) through a triphosphate linkage (Figure 2(b)). To examine whether the same activity of NSP2 responsible for hydrolyzing the γ-phosphate from the [^{32}P]5′g8 RNA could also hydrolyze the triphosphate linkage of the cap, we

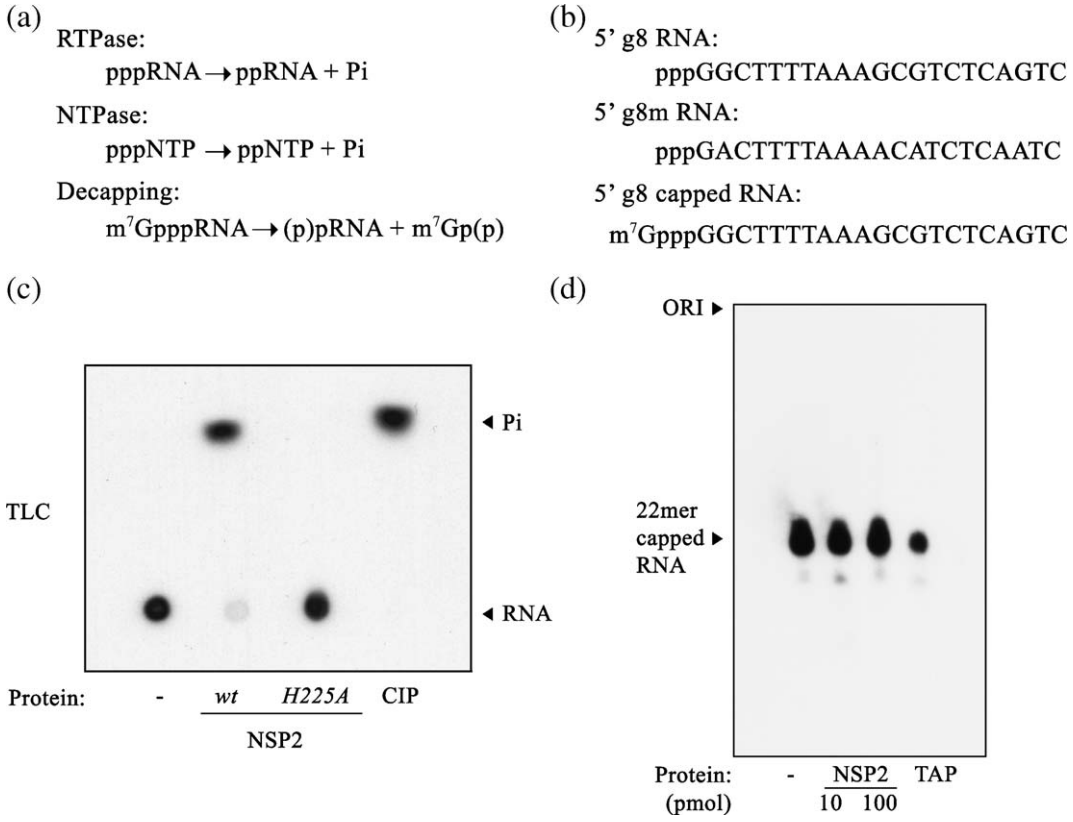

Figure 2. NSP2 removes the γP from RNA. (a) Substrates and products catalyzed by different activities. (b) Sequences of RNA probes used in RTPase and decapping assays. (c) Removal of the γP (P_i formation) from [γ-^{32}P]5′g8 RNA by wtNSP2 (wt) and an NTPase-defective mutant, H225A, in reaction mixtures containing 7 pmol protein and 14 pmol of probe was examined by TLC. Control reactions contained no protein (lane 1) or calf intestinal phosphatase (CIP) (lane 4). (d) Decapping activity was analyzed in reaction mixtures containing 10 pmol or 100 pmol of *wtNSP2* and 10 pmol of ^{32}P-labeled 5′g8 capped RNA. Control reactions contained no protein (lane 1) or tobacco acid pyrophosphatase (TAP) (lane 4). Radiolabeled products were analyzed by electrophoresis on a polyacrylamide gel containing 7 M urea.

prepared a capped g8 RNA probe ([^{32}P]5′g8 capped RNA) that was radiolabeled specifically at the phosphate group immediately adjacent to the inverted guanosine (Gp*ppGGC..., radiolabeled residue denoted with an asterisk). Incubation of *wtNSP2* with [^{32}P]5′g8 capped RNA failed to disrupt the cap structure (Figure 2(d)), even under conditions in which the amount of protein to probe was vastly in excess over that required to completely remove the γ-phosphate from uncapped ^{32}P-5′g8 RNA (10:1) (Figure 2(c)). These results indicate that capped RNAs are not substrates of the RTPase-like activity of the NSP2 octamer.

To determine whether the activity of NSP2 was limited strictly to removing the γP, or included removing all three phosphates (γ, β, α) from the 5′ end of an uncapped ssRNAs, *wtNSP2* octamers were incubated with [γ-^{32}P]5′g8m RNA and with a second related RNA labeled only at its 5′-terminal αP position with ^{32}P ([α-^{32}P]5′g8m RNA) (Figure 2(b)). The 5′g8m RNA is the same as the 5′g8 RNA except that all its guanine residues but that at the +1 position were replaced with adenine, thereby allowing labeling of only the αP of the +1G when the RNA was made in the presence of [α-^{32}P]GTP. The products were assayed for the formation of $^{32}P_i$ by TLC (Figure 3(a)) and for the loss of radiolabel from the RNA by gel electrophoresis (Figure 3(b)). The results showed that NSP2 caused the release of $^{32}P_i$ from the [γ-^{32}P]5′g8m RNA, but did not remove label from the [α-^{32}P]5′g8m RNA. Its failure to remove the αP excludes the possibility that NSP2 can cleave the 5′-terminal phosphoester bond of the RNA, thereby indicating that NSP2 does not have phosphatase activity.

To address whether NSP2 could cleave the 5′ β–α phosphoanhydride bond of an RNA, [α-^{32}P]5′g8m RNA was incubated in the presence and absence of *wtNSP2*. Afterwards, the reaction mixtures were incubated with RNase T1 to allow complete hydrolysis of the RNA to nucleotides. TLC was then used to analyze the mixtures for ^{32}P-labeled-derivatives of the 5′-terminal guanosine (p*Gp, pp*Gp, and ppp*Gp). The results showed that in the absence of *wtNSP2*, only ppp*Gp was recovered from reaction mixtures, a result consistent with the location of the polyphosphorylated nucleoside at the +1 position of the RNA molecule (Figure 3(c)). In reaction mixtures containing *wtNSP2*, pp*Gp was the only radiolabeled product detected. A comparison of the products of the two reaction mixtures indicates that *wtNSP2* catalyzed the removal of the γP but not the βP from the RNA. Thus, NSP2 is an RTPase, as

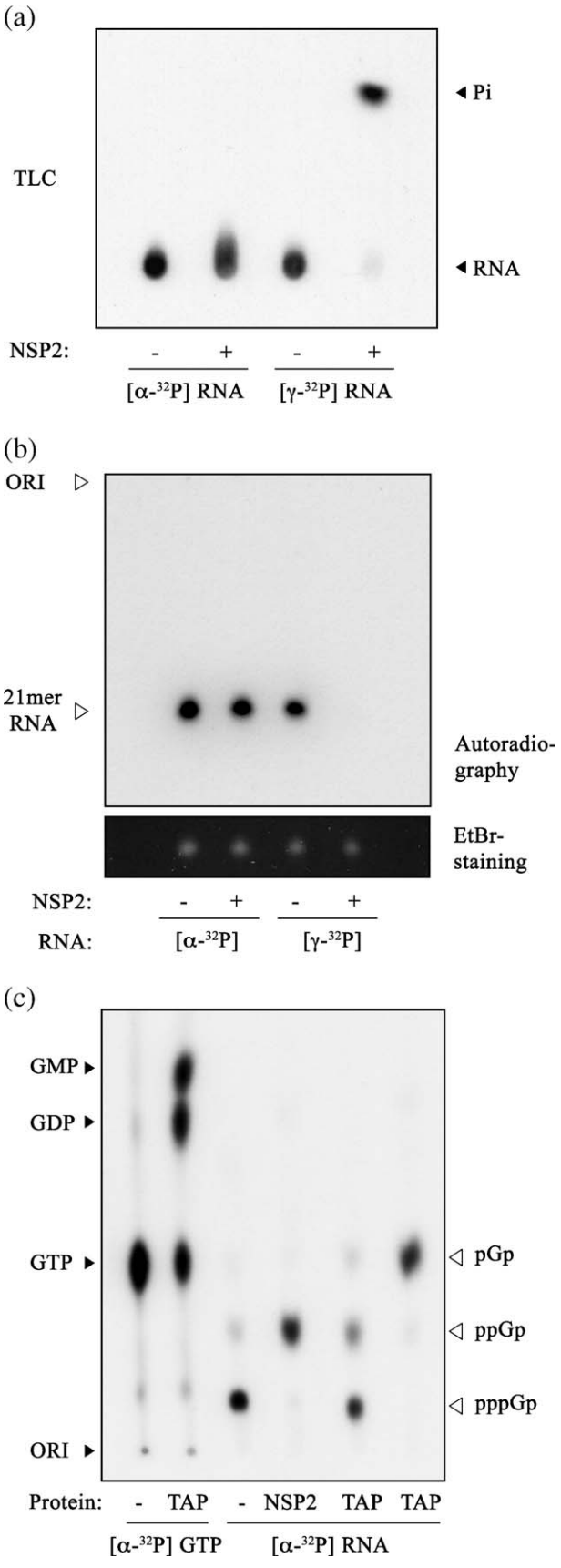

Figure 3. NSP2 targets the γ-β phosphoanhydride bond of RNA. (a) and (b) Reaction mixtures of RTPase assays performed with [γ-^{32}P]- or [α-^{32}P]5′g8m RNA (21-mer) and wtNSP2 were analyzed for P_i formation by TLC (a) and for ^{32}P-labeled RNA by electrophoresis on a 7 M urea–polyacryamide gel (b) and autoradiography. The portion of the gel containing RNAs, stained with ethidium bromide, is also shown (b). (c) Reaction mixtures of RTPase assays performed with [α-^{32}P]5′g8m RNA were digested with RNase T1, then resolved by TLC. Markers were prepared by partial (lane 2 and 5) or complete (lane 6) digestion of [^{32}P]GTP and [α-^{32}P]5′g8m RNA with TAP.

its activity is limited to cleaving the γ-β phosphoanhydride bond.

Kinetics of RTPase activity

The formation of $^{32}P_i$ in RTPase assays as a factor of time and of protein concentration was analyzed by TLC and quantified with a phosphorimager. The results showed that in assays containing 7 pmol of *wtNSP2* monomer and 14 pmol of [γ-^{32}P]5′g8 RNA, near complete hydrolysis (~90%) of the substrate was achieved by 60 min, with a 50% value reached by ~15 min (Figure 4(a)).

To calculate V_{max} and K_m values for the RTPase activity, reaction mixtures containing NSP2 and increasing concentrations of [γ-^{32}P]5′g8 RNA were incubated for 15 min, then analyzed for the presence of P_i. A Michaelis-Menten plot of the RNA substrate concentration versus rate of P_i formation indicated a V_{max} of 21 fmol/min for the RTPase activity (Figure 4(b)). This value is remarkably similar to that (18 fmol/min) reported earlier for the NTPase activity of NSP2 (Table 1).[18] In comparison, the K_m value calculated for the RNA substrate of the RTPase activity (0.038 μM) was 17-fold lower than the K_m value reported earlier for the NTP substrate of the NTPase activity (0.65 μM) (Table 1). Thus, NSP2 has a significantly higher affinity for the substrate of its RTPase activity than its NTPase activity, consistent with the RNA-binding activity of the octamer grooves.

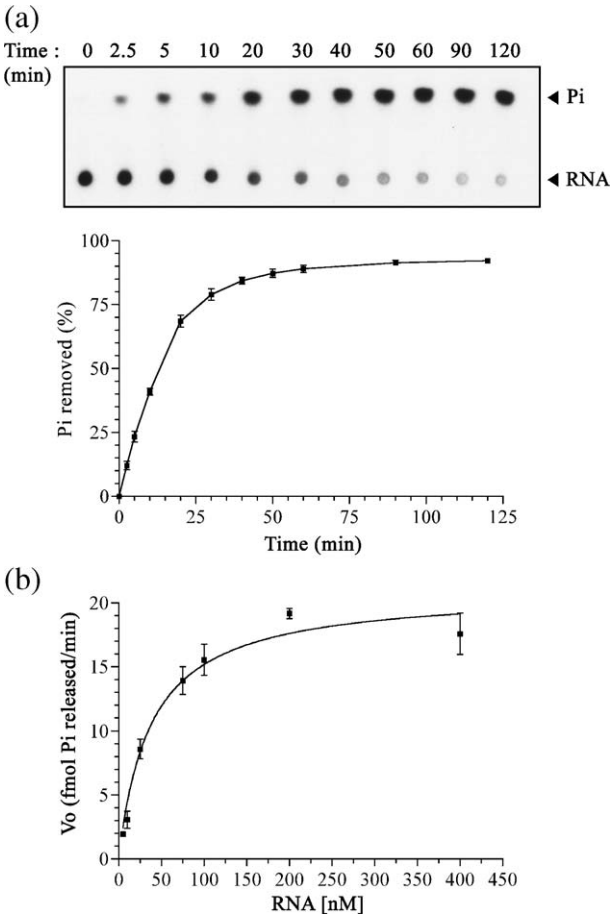

Figure 4. Properties of the RTPase activity. The formation of P_i in RTPase assays as a factor of time (a) and substrate (b) concentration was analyzed by TLC, and quantified with a phosphorimager. (a) Reaction mixtures contained 7 pmol of wtNSP2 and 14 pmol of[γ-^{32}P]5′g8 RNA. (b) Reaction mixtures (10 μl) contained 1 pmol (0.1 μM) of wtNSP2 and increasing concentrations (0 to 0.4 μM) of [γ-^{32}P]5′g8 RNA, and were incubated for 15 min. Initial velocities (Vo) were determined from slopes calculated from the initial linear points of the curve generated from plotting P_i formation *versus* time (a). Error bars represent the standard deviations of two or more experiments.

RTPase mediated NSP2 phosphorylation

A characteristic of the NTPase activity of NSP2 is that the γP cleaved from the NTP molecule is covalently transferred to the catalytic His225 residue, producing a phosphorylated intermediate.[16,18,21] To determine whether cleavage of the γP of an RNA was likewise associated with the phosphorylation of the protein, *wtNSP2* and *H225A* were incubated with [γ-^{32}P]5′g8 RNA in RTPase assays. The reaction mixtures were analyzed for radiolabeled protein by SDS-PAGE and autoradiography. The results showed that *wtNSP2* underwent phosphorylation during the hydrolysis of the γ–β phosphoanhydride bond of the RNA, whereas the enzymatically-inactive *H225A* did not (Figure 5). These data indicate that the RTPase and NTPase activities of NSP2 are mediated by the same catalytic site, both employing a hydrolysis mechanism leading to NSP2 phosphorylation.

Substrate competition between RTPase and NTPase activities

The importance of His225 not only to the RTPase and NTPase activities of NSP2 but also to the phosphorylation of the protein, combined with the similarity of the V_{max} values of these activities, suggests that the same catalytic site directs the hydrolysis of the γ–β phosphoanyhydride bond of RNAs and NTPs. To examine this possibility further, we performed competition experiments that measured how the addition of GTP, GDP, or GMP to reaction mixtures containing *wtNSP2* and [γ-^{32}P]5′ g8 RNA affected RTPase activity. The results showed that at high molar ratios of GTP to the RNA substrate, GTP successfully inhibited RTPase activity in a concentration dependent manner (Figure 6). The fact that a 50% reduction in $^{32}P_i$ formation required a ratio of RNA to GTP of 1:2500–3000 may reflect, in part, the higher affinity of NSP2 for the RNA substrate of its RTPase activity as compared to the affinity of NSP2 for the NTP substrate of its NTPase activity. Competition assays performed with GDP showed that this nucleotide was approximately one-third as effective in reducing $^{32}P_i$ formation as GTP, producing a 50% reduction in RTPase activity at a ratio of RNA to

Table 1. Kinetic parameters of viral RTPases/NTPases

Virus	Protein	RTPase		NTPase		References
		V_{max} (fmol min^{-1})	K_m (μM)	V_{max}[c,d] (*x*mol min^{-1})	K_m^d (μM)	
Alphavirus SFV[a]	NSP2	55	2.99	2.3 pmol	90	42
Reovirus	λ1	57	0.26	0.23 pmol	1	53, 54
Reovirus	μ2	36	0.32	2.4 nmol	2500	46
Rotavirus	NSP2	21[b]	0.038[b]	18.0 fmol	0.65	This study, 18
Vaccinia virus	D1	50 pmol	1.00	0.61 nmol	800	33

[a] Semlike Forest virus.
[b] The values for V_{max} and K_m were determined from calculation of hyperbolic fits to the Michaelis-Menten equation by non-linear regression using Prism 3.0 (GraphPad Software).
[c] *x*mol represents nmol, pmol, or fmol, as indicated.
[d] V_{max} and K_m values correspond to the values obtained with ATP as a substrate, except for the case of SFV were the values correspond to GTPase activity.

GDP of ~1:6000. In contrast to GTP and GDP, GMP had little or no effect on the RTPase activity even at very high concentrations. These results indicate that GTP, and to a lesser extent GDP, compete with ssRNA as substrates for hydrolysis, supporting the concept that a common active site directs both the RTPase and NTPase activities of NSP2. The fact that a high concentration of nucleotide relative to RNA is required to reduce RTPase levels supports the concept that RNA is the preferred substrate of NSP2.

Relationship between RNA binding and substrate preference

The four highly basic grooves that span the periphery of the NSP2 octamer are binding sites for ssRNA.[14,22] Each groove is positioned at the tetramer–tetramer interface such that it spans across two catalytic clefts, each in an opposing tetramer unit (Figure 1(b) and (c)). This structural arrangement raises the possibility that binding of RNA to the groove, enhances the RTPase activity of the octamer by recruiting the substrate for the reaction to a position near the catalytic site. In order to test this possibility, two mutant species of the NSP2 octamer were prepared, in which either three (*mt3Q* (Lys59, Arg60, Arg68)) or six (*mt6Q* (Lys37, Lys38, Lys58, Lys59, Arg60, Arg68)) conserved and solvent-exposed electropositive residues along the grooves and proximal to the catalytic clefts were replaced with glutamine, a polar non-charged amino acid (Figures 1(d) and 7(a)). The sedimentation properties of the charge-deletion mutants, *mt3Q* and *mt6Q*, were indistinguishable from that of *wtNSP2*, an indication that the mutant forms retained the octamer configuration (data not shown). However, the extent to which glutamine-mutagenesis may have induced structural changes near the catalytic clefts that indirectly perturbed the activities of *mt3Q* and *mt6Q* remains unresolved.

The RNA-binding activities of *mt3Q* and *mt6Q* were assessed by electrophoretic mobility shift assay (EMSA) and by poly(U)-Sepharose binding assay. EMSA performed by incubating the non-viral RNA probe, ^{32}P-labeled Luc200, with wild-type and mutant proteins indicated that the mutations in *mt3Q* and *mt6Q*, although not abolishing RNA-binding activity, reduced their levels (Figure 7(b)). This was most apparent in reaction mixtures

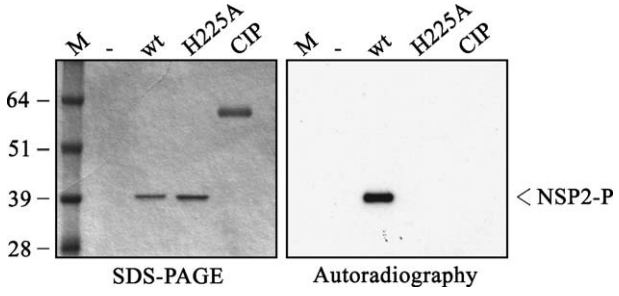

Figure 5. RTPase activity produces a phosphorylated NSP2 intermediate. Reactions mixtures from RTPase assays containing [γ-^{32}P]5′g8 RNA and *wtNSP2* or the mutant *H225A* were incubated for 1 h at 37 °C. Control reactions contained CIP or no protein. Protein in the mixtures were resolved by gel electrophoresis and detected by Coomassie blue staining and autoradiography. NSP2-P, phosphorylated NSP2; M, protein marker.

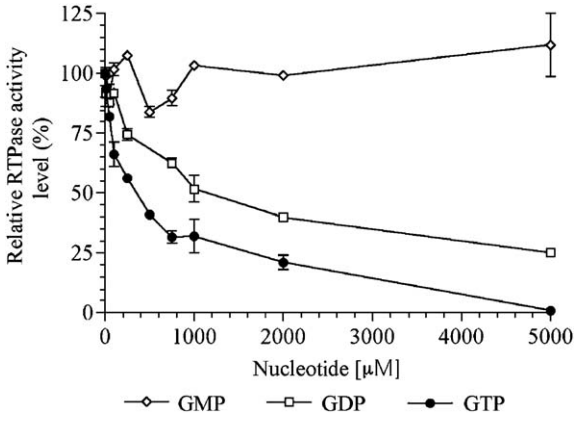

Figure 6. GTP competitively interferes with RTPase activity. Reactions containing 50 mM Tris–HCl, 2 mM $MgCl_2$, 150 nM [γ-^{32}P]5′g8 RNA, 1 pmol NSP2 and 0 to 5 mM GTP, GDP or GMP, were incubated at 37 °C for 25 min. P_i formation was detected by TLC and quantified with a phosphorimager.

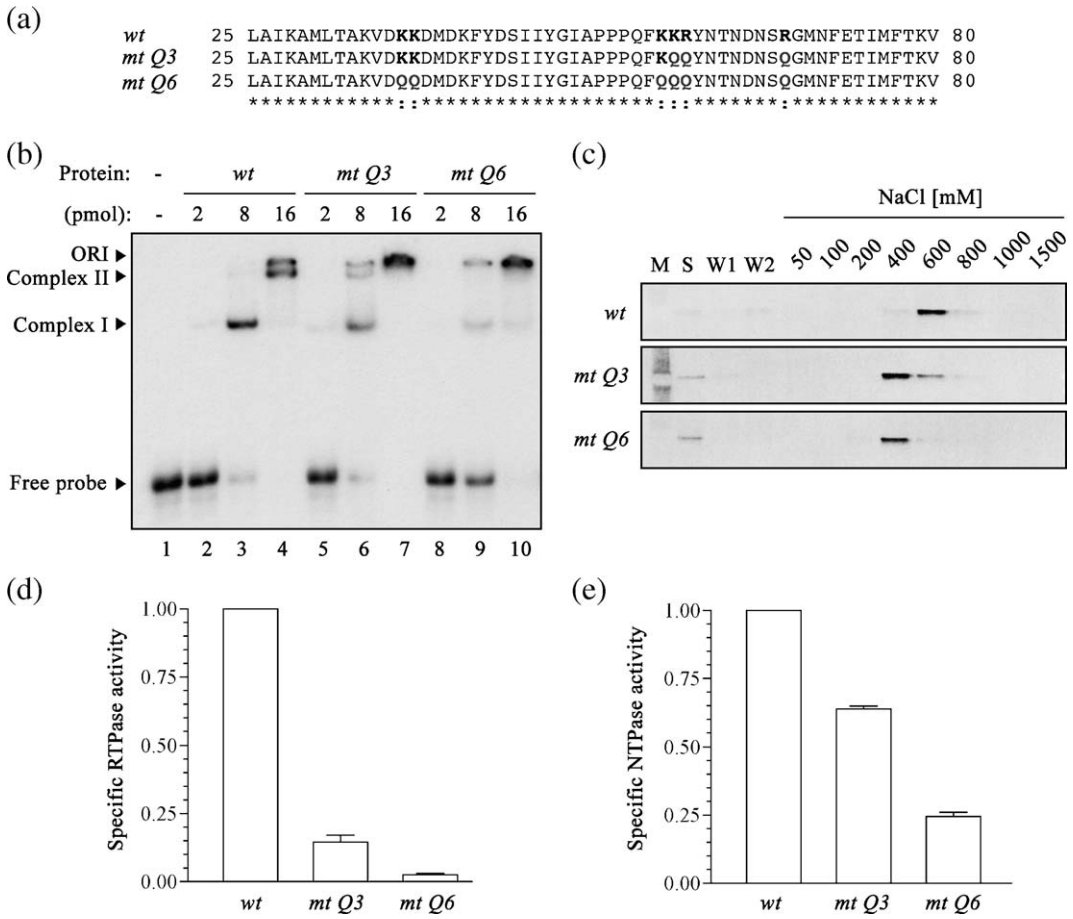

Figure 7. Relationship between the RNA-binding and RTPase activities of NSP2. (a) Partial NSP2 sequence alignment indicating electropositive residues subjected to glutamine mutagenesis. (b) Complexes formed by incubating wild-type and mutant forms of NSP2 with ^{32}P-labeled Luc200 RNA were detected by non-denaturing gel electrophoresis (EMSA) and autoradiography. (c) Wild-type and mutant forms of NSP2 bound to poly(U)-Sepharose beads were eluted by stepwise exposure to increasing concentrations of NaCl. Protein eluted from the beads was detected by SDS-PAGE and silver staining. (d) RTPase assays were performed by incubating (γ-^{32}P)- labeled g8-5′ RNA with increasing concentrations of wild-type and mutant NSP2 (7, 14, and 28 pmol) for 20 min. (e) NTPase assays were performed by incubating [γ-^{32}P]ATP with increasing concentrations of wild-type or mutant NSP2 (14, 28, and 42 pmol) for 1 h. P_i formation was detected by TLC ((d) and (e)), and quantified with a phosphorimager. Specific activities were calculated as product formation (pmol of P_i) per quantity of the protein in the reaction. Results are presented as a percentage of the value obtained for the reactions containing the wild-type protein.

containing 8 pmol of protein, which showed that mutations in *mt3Q* and *mt6Q* caused reductions in the formation of the simplest octamer–probe complex (complex I) of ~35 and 80%, respectively. Similarly, mutations in the *mt3Q* and *mt6Q* did not prevent these proteins from binding to poly(U)-Sepharose. But based on salt-elution profiles, the mutations did decrease the strength of the interaction between the octamer and RNA (Figure 7(c)). These data suggest that the mutated residues of *mt3Q* and *mt6Q* contribute to the RNA-binding activity of NSP2, but in addition, point out that other residues are involved in this activity as well.

Comparison of the RTPase activities of *wtNSP2*, *mt3Q*, and *mt6Q* showed that mutation of conserved electropositive residues along the grooves significantly reduced formation of P_i from [γ-^{32}P]5′g8 RNA (Figure 7(d)). In particular, glutamine mutagenesis of the three residues Lys59, Arg60, and Arg68 caused a five- to tenfold decrease in activity. These mutations combined with those of Lys37, Lys38, and Lys58 reduced the activity even further, such that the amount of substrate hydrolyzed by *mt6Q* was 20-fold or less than that hydrolyzed by *wtNSP2*. These data indicate that mutation of residues affecting the RNA-binding activity of the octamer had a strong effect on RTPase activity, pointing to an interdependency of these two activities.

In NTPase assays, both *mt3Q*, and *mt6Q* showed reduced levels of activity, but to degrees much less than observed for their RTPase activities (Figure 7(e)). For instance, although the RTPase activity of *mt3Q* was reduced by five- to tenfold, its NTPase activity was reduced by less than twofold. And while the RTPase activity of *mt6Q* was decreased by 20-fold or more, its NTPase activity was decreased by fourfold. The reduction in NTPase

activity most likely stems from the decreased affinity of NSP2 for NTPs due to the charge-deletion mutations of *mt3Q* and *mt6Q* perturbing the electropositive zone around the entrance to the catalytic cleft.

Modeling of RNA interaction with the cleft

To gain further insight into the interaction of ssRNA with the catalytic cleft, multiple RNA docking simulations were performed using Autodock 3.02 to predict the interaction of a five base RNA (pppGGCUU) with NSP2. Among the most favored energetic positions (lowest energy) were those suggesting the insertion of the 5′ end of the RNA deep within the cleft, with its 5′-terminal triphosphate group situated in the active site. The remainder of the RNA was oriented such that its 3′ end extended from the cleft. One representative position was selected and subjected for molecular dynamics simulation using CHARMM to define possible interactions formed between the protein and the ligand. The results suggested that several electropositive residues in the RNA-binding loop interacted with the 5-mer RNA, including residues shown above to be important in the RNA-binding and RTPase activities of NSP2 (Figure 8(a)). Analysis of the RNA–protein complexes after simulation indicated a web of interactions (mainly hydrogen bonds) between Lys59, Arg60, and Arg68 and the oxygen moieties present at positions three and four of the RNA molecule backbone (third and fourth nucleoside) (Figure 8(b)). The simulation also indicated that Lys37 interacted with the fifth position of the RNA (last nucleoside). The simulation failed to suggest any interaction between Lys38 and Lys58 and the RNA. A remarkable suggestion of the simulation was the interaction of the 5′-terminal triphosphate group of the RNA with the catalytic residue His225 and other residues involved in the NTPase activity (Figure 8(c)).[18] In summary, the results obtained by the RNA simulation suggest that several of the basic residues selected for charge-deletion mutation in *mt3Q* and *mt6Q* may have an effect on directing and stabilizing the 5′ end of RNA in the cleft such that its terminal phosphate bond is appropriately oriented for nucleophilic attack.

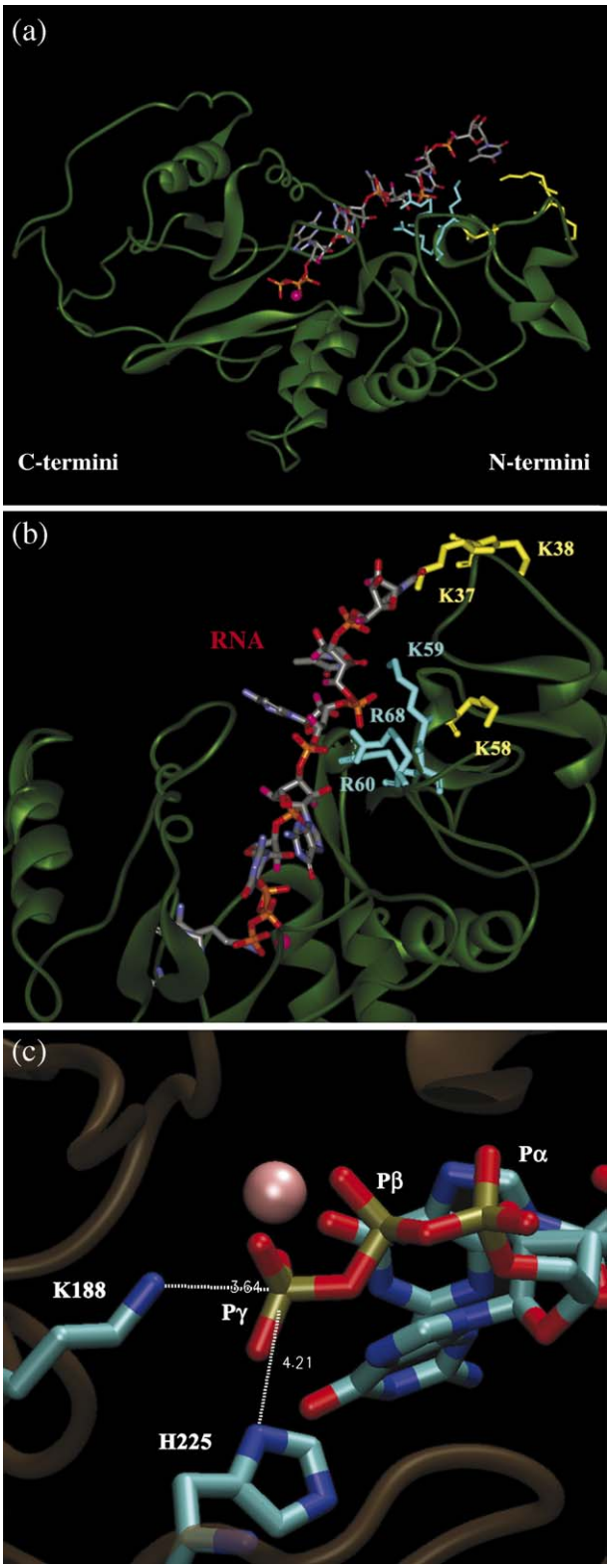

Figure 8. Modeling at the interaction of RNA with the cleft of NSP2. One representative RNA docking position was chosen and further subjected to molecular dynamics for 1 ns using CHARMM. After stabilization of the system (1 ns), the RNA–protein complex was analyzed for ligand–enzyme interactions. Modeling of RNA docking in NSP2 predicted the binding of the 5′ end of the RNA molecule deep inside the cleft and the rest of the molecule (third and fourth nucleotides) interacting with the basic residues located outside of the CLEFT ((a) and(b)). Basic residues previously selected for mutagenesis are denoted in cyan (K^{59}, R^{60}, R^{68}) and yellow (K^{37}, K^{38}, K^{58}). Colors assigned to the RNA molecule are in CPK. (c) Close up view of the triphosphate at the 5′ end of the RNA molecule. Two critical residues for the NTPase/RTPase activity located at the active site are shown. Distances between the γP at the 5′ end of RNA and two residues from the active site are shown in Angstrom units. The Mg^{2+} is shown as a pink sphere.

Effect of NSP5 on NSP2 RTPase activity

The charge complementarity of the basic NSP2 and the acidic NSP5 may contribute importantly to the interaction of these proteins, and therefore, to the formation of viroplasms. Indeed, cryo-electron microscopy has indicated that a truncated species of NSP5 binds to NSP2 along the same electropositive grooves involved in the association of RNA with NSP2.[22] Given the shared affinity of RNA and NSP5 for the grooves of the octamer, NSP5 may reduce RTPase activity by interfering with the ability of NSP2 to recruit the RNA substrate of the reaction. To examine this possibility, full-length NSP5 with an N-terminal His tag was expressed in bacteria and purified by Ni^{2+}-affinity chromatography. The recombinant NSP5 (*wtNSP5*) was combined with *wtNSP2* or the glutamine mutants *mt3Q* or *mt6Q*, and the mixtures then incubated with [γ-^{32}P]5′g8 RNA under RTPase assay conditions. Analysis of the reaction products showed that the presence of *wtNSP5* did not measurably affect the amount of $^{32}P_i$ formed in any of the assays (Figure 9), a result suggesting that NSP5 did not impede the binding of the RNA substrate to the octamer nor alter the hydrolysis activity of the HIT-like motif.

Importance of electropositive residues on viroplasm formation

Transient expression of NSP2 and NSP5 in mammalian cells results in the formation of viroplasm-like structures (VLSs).[8] To examine whether the same electropositive residues shown above to influence the RNA-binding and RTPase activities of NSP2, also affected the ability of NSP2 to form viroplasms, we co-expressed non-histidine tagged versions of *wtNSP2*, *mt3Q* and *mt6Q* with NSP5 in MA104 cells. Immunofluorescence analysis of these cells using NSP2 and NSP5-specific antisera revealed that the charge-deletion mutations in *mtQ3* had only a partial effect on the ability of the protein to support the formation of VLSs (Figure 10). In particular, while *mt3Q* supported VLS formation, these inclusions were generally smaller than those formed with *wtNSP2*, and there was a conspicuous increase in the amount of NSP2 and NSP5 distributed throughout the cytosol, that failed to localize to viroplasms. In contrast, the mutations in *mtQ6* prevented this protein from supporting the formation of VLSs. Instead of localizing to inclusions, *mtQ6* and NSP5 were distributed throughout the cytosol in a manner that was only partially overlapping, with *mt6Q* having a somewhat granular appearance. Thus, in addition to the importance of the electropositive residues adjacent to the groove in the RTPase and RNA-binding activities of NSP2, these residues have critical function in the formation of viroplasms. Most likely, the charge-deletion mutations of *mt3Q* and *mt6Q* altered the surface charge of NSP2 in such a way that the protein could no longer interact appropriately with NSP5 to support viroplasm formation. Alternatively, the charge-deletion mutations prevented NSP2 from binding RNA, and therefore prevented the RNA-mediated bridging of NSP2 and NSP5 that may have a role in viroplasm formation. The failure of viroplasms to form with the *mt3Q* and *mt6Q* species is not due to their failure to efficiently hydrolyze the γ–β phosphoanhydride bond of RNA, since previous studies showed that the NTPase and RTPase-defective mutant *H225A* supported the formation of viroplasms as efficiently as *wtNSP2*.[18]

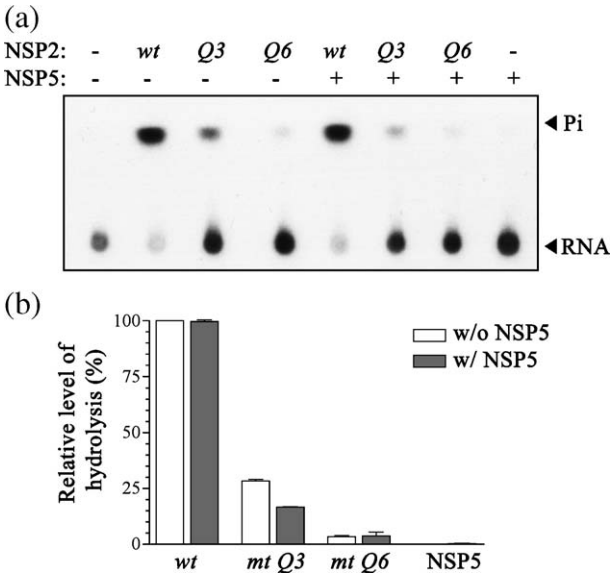

Figure 9. NSP5 does not have an inhibitory effect on NSP2 RTPase activity. Reaction mixtures containing 14 pmol of (γ-^{32}P)- labeled g8-5′ RNA, 0.2 mM $MgCl_2$, 14 pmol of NSP5 and 7 pmol of *wt* or *mt* NSP2 were incubated for 1 h at 37 °C. P_i formation was detected by TLC and autoradiography (a) and quantified by phosphorimager (b). Levels of hydrolysis were normalized respect to the value obtained for *wt* NSP2 in absence of NSP5 and set as 100%. Error bars represent the standard deviation of two experiments.

Discussion

Our results show that the rotavirus NSP2 octamer can hydrolyze the γ–β phosphoanhydride bond of an RNA, thus defining the protein as an RTPase. This activity is indistinguishable from that of the NTPase activity of NSP2, both representing metal-dependent hydrolysis reactions with similar V_{max} values that require the H^{225} residue and that produce a phosphorylated enzyme intermediate and free P_i. These results and those of competition assays indicate that hydrolysis of the RNA and NTP substrates occur at a common active site, located within a deep electropositive cleft of each NSP2 monomer. The cleft includes features characteristic of HIT proteins including a fold that is similar to one present in the catalytic core of PKCI and a HIT-like active site. Although NSP2 can

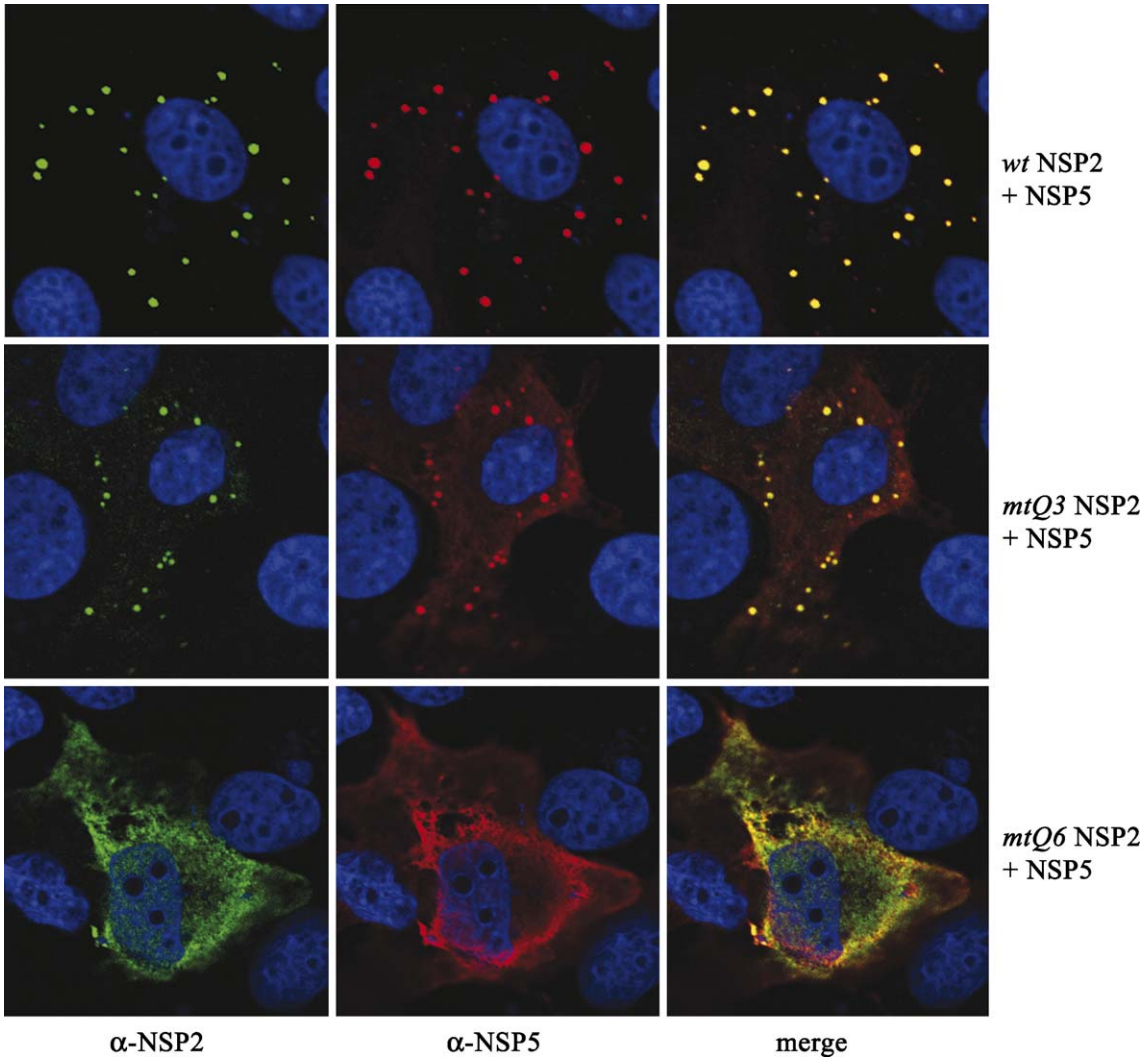

Figure 10. RTPase defective NSP2 mutants are deficient in the formation of VLS in transfected mammalian cells. MA104 cells were transfected with pCI vectors encoding *wt* or *mt* forms of NSP2 and/or NSP5. Localization of proteins was detected using NSP2 and NSP5 specific antisera in combination with fluorescent dye labeled secondary antibodies. Alexa 488 (green) and Alexa 594 (red) were used to detect NSP2 and NSP5, respectively. Nuclei were visualized by staining with DAPI. Immunostained cells were analyzed by confocal laser scanning microscopy. Co-localization of the proteins is observed by yellow color in the superimposed images (right panel).

remove the γP from either RNA or NTP, RNA represents the preferred substrate due to the higher affinity (K_m) of the octamer for this molecule. In comparison to other known viral RTPases, the K_m value indicates that the NSP2 octamer has a remarkably strong affinity for its RNA substrate (Table 1), suggesting that this represents a legitimate catalytic activity of the protein during the viral life cycle.

The fact that NSP2 accumulates in specialized structures (viroplasms) in the infected cell in which viral RNAs are made and concentrated indicate that NSP2 functions in an environment that contains the substrates for both its NTPase and RTPase activities.[7,9] In the viroplasm, the high affinity of NSP2 for its RNA substrate may enable the octamer to switch readily from a default NTPase function to an RTPase function, even in a nucleotide-rich environment. The results of a recent study suggest that the default (RNA-free) function of the NSP2 octamer may be to act as an independent NTP generation system in the viroplasm, whereby the NTPase activity of the protein produces the P_i required by its associated kinase activity to recycle spent NDPs back to NTPs.[21] In the presence of RNA substrate, the low K_m value of its RTPase activity could be anticipated to induce NSP2 to switch from such an NTPase/NDP kinase function to an alternative function more directly linked to RNA replication, translocation, or packaging.

During rotavirus replication, viral (+)-strand RNAs serve as templates for (−)-strand synthesis, yielding dsRNA products. The (+) strand of the dsRNA products have a 5′-methylated cap, while the (−) strand is uncapped, ending instead with a β–α phosphorylated 5′-guanosine.[23,24] The absence

of a γP on this residue raises the possibility that during replication, NSP2 uses nascent (−)-strand RNAs as substrates for its RTPase activity. Indeed, earlier studies have indicated that NSP2 is a component of viral replication intermediates, interacts with the RdRP VP1, and is bound to partially replicated RNA, features that are consistent with the direct participation of NSP2 in (−)-strand synthesis.[5,11–13] One possibility is that soon after (−)-strand initiation, the nascent RNA product interacts with NSP2 in such a way that its 5′ end enters into one of the clefts of an octamer, where it engages the active site. This interaction may anchor the nascent (−) strand as the RdRP carries out elongation. As the RdRP nears completion of the (−) strand, the affinity of the RdRP and NSP2 for each other, combined with the interaction of NSP2 with the 5′ end of the (−) strand, and the interaction of the RdRP with the 3′ end of the (−) strand may generate a complex in which the dsRNA product is circularized. Interestingly, the high efficiency of transcription by DLPs has led to the suggestion that the dsRNAs are circularized within the capsid, an organization allowing the polymerase to move expeditiously from the 5′ to the 3′ end of the (−)-strand template following rounds of (+)-strand synthesis.[25,26] The NSP2–RdRP -mediated bridging of the ends of the dsRNA product may be responsible for initially establishing the circularized form of the genome segments.

Through its affinity for ssRNA, NSP2 can be expected to form complexes with the (+)-strand RNAs that accumulate in viroplasms. Despite such interactions, our *in vitro* assays indicate that NSP2 cannot use methylated capped (+)-strand RNAs as substrates for hydrolysis. Interestingly, one of the well-characterized HIT-family proteins, DcpS, possesses a 7-methyl guanosine specific hydrolase activity that is responsible for mRNA decapping during exosome-mediated decay.[27] The failure of NSP2 to utilize a methylated capped RNA as a substrate for hydrolysis despite sharing a HIT-like motif and a HIT-like fold similar to those of DcpS, may have multiple explanations. Perhaps most importantly is the observation that in the HIT site of DcpS, side-chain interactions are established that mediate the specific recognition of methylated guanosine residue of the cap structure, and as consequence, the engagement of the phosphate residues of the cap structure with the catalytic residues of the active site.[28] It should also be noted that DcpS, like other HIT proteins, exists as an asymmetric dimer when bound to a cap, a conformation that leaves its catalytic cleft in a structurally open and solvent accessible form.[28] In contrast, NSP2 is an octamer with a 4-2-2 symmetry, in which substrate binding and hydrolysis occur within the deep clefts that divide each monomer. In contrast to the openness of the HIT site of DcpS, the constrained accessibility and rigidity of the deep clefts in the NSP2 octamer may restrict capped RNAs from gaining entry to the HIT site. It is also possible that the NSP2 cleft may not have appropriate dimensions to spatially accommodate the inverted guanosine of the cap in such a way that the triphosphate linkage can engage the catalytic residues needed for nucleophilic attack. The lack of a common substrate between proteins in the large HIT superfamily despite shared catalytic HIT motif and a C-terminal HIT fold in their structures has been reported.[20]

Interestingly, NSP2 is the only rotavirus protein known to have an RTPase activity, an observation that could be interpreted to mean that NSP2 participates in the capping process by removing the γP from RNA prior to guanylylation. However, this possibility can be excluded, since NSP2 is not a component of the transcriptionally active DLPs that produce the ^{m7}GpppG-capped (+)-strand RNAs.[29] More likely, the capping–related RTPase activity is provided by VP3, a protein within DLPs shown previously to have guanylyltransferase and methyltransferase-like activities.[30,31] In cell-free replication assays, where VP1 can carry out (−)-strand initiation and elongation, the γP is not removed from the (+)-strand template, indicating that the rotavirus RdRP lacks RTPase activity and that there is not a direct need for an RTPase activity in the polymerization of the (−)-strand.[32]

Transient expression of NSP2 and NSP5 leads to the formation of inclusion bodies that are similar to those that form in rotavirus-infected cells.[8] In our analysis, we found that the formation of such VLSs was abrogated when NSP2 was replaced with the glutamine charge-deletion mutant *mtQ6*. Although *mtQ6* is defective in RTPase activity, and to a lesser extent in NTPase activity, it is unlikely that these deficiencies contributed to the defect in VLSs formation, given the results of an earlier study showing that the catalytically inactive NSP2 mutant *H225A* supported inclusion formation.[18] Instead, it is more likely that *mtQ6* failed to support VLSs formation because of the loss of critical electropositive charges needed to support its stable interaction with the acidic protein NSP5 or with ssRNA, or a combination of the two. Because NSP2 and NSP5 both have affinity for ssRNA,[13,47] mutations that reduce the RNA-binding activity of NSP2 may also interfere with viroplasm formation by preventing effective RNA-mediated bridging of NSP2 and NSP5.

Cellular and viral RTPases can be divided into two groups based on their catalytic requirement for a divalent cation. Metal-dependent RTPases have been described for metazoan DNA viruses (e.g. Poxvirus, *Chlorella* virus), fungi, and protozoan parasites.[33,34] These RTPases are known to remove the γP from not only RNAs, but also NTPs, *via* hydrolysis reactions taking place at a common active site. The X-ray structure of the *Sacharomyces cerevisiae* Cet 1 RTPase suggests that the active site of the fungal and *Chlorella* virus enzymes is contained in an open hydrophilic tunnel formed by eight antiparallel β-strands, in which two conserved glutamates residues are critical for hydrolysis of the γ-β phosphate bond.[34,35] Metal-independent

RTPases have been identified in mammals and other metazoan organisms. Characteristically, these RTPases undergo phosphorylation during the hydrolysis reaction due to the transfer of the γP to a residue at the active site (e.g. phosphotyrosine). These RTPases are usually incapable of using NTPs as substrates.[36] The recently solved structures of mouse Mce1 and *Baculovirus* BVP RTPases suggests the existence of another class of RTPases, wherein the active site is located at the bottom of a deep positively charged pocket containing a conserved cysteine residue that acts as the catalytic amino acid.[37,38] Several other enzymes with dual RTPase and NTPase activities have been identified, including some belonging to RNA virus families (e.g. NS3 of dengue virus, NS13 of coronavirus, Nsp2 of alphavirus).[39–42] The relationship of these dual functioning enzymes, if any, to previously described RTPases is uncertain, in part due to the lack of sufficient biochemical and structural information.

Rotavirus NSP2, with its novel HIT-like fold and motif, is the only solved RTPase/NTPase of a dsRNA virus. Other viruses belonging to the *Reoviridae* family encode non-structural proteins with characteristics similar to that of NSP2, including the well-studied NS2 protein of bluetongue virus (BTV) and σNS protein of orthoreovirus.[43] Like the NSP2 protein, NS2 and σNS self-assemble into homomultimeric complexes with associated ssRNA-binding and helix-unwinding activities and are components of viral replication intermediates.[43–45] Furthermore, both NS2 and σNS participate in viroplasm formation in BTV- and reovirus-infected cells, respectively. In contrast to the RTPase/NTPase activity of rotavirus NSP2, BTV NS2 has an associated phosphatase activity, allowing it to remove all three phosphates from an NTP. Unlike NSP2 and NS2, σNS has no known enzymatic activity. However, during assembly of viroplasms in reovirus-infected cells, σNS interacts with μ2, a non-structural protein with RTPase/NTPase activity.[46] Thus, a common feature of *Reoviridae* viroplasms appears to be the presence of non-structural proteins with catalytic activity capable of hydrolyzing phosphate groups from NTPs, and in at least some cases, from the 5′ end of ssRNAs. Despite their related activity, only rotavirus NSP2 is known to contain a HIT-like fold and motif, and hence its mechanism of hydrolytic attack can be expected to unlike that of NS2 and σNS.

The unique combination of properties in NSP2, *vis-à-vis*, metal-dependent hydrolysis within a deep electropositive cleft mediated by His residues that results in the transient phosphorylation of the enzyme, establish rotavirus NSP2 as new class of NTPase/RTPases. Given the importance of the catalytic activity of NSP2 in rotavirus replication, the development of antiviral compounds (e.g. nucleotide analogs) that target the activity of NSP2 HIT site should be considered as an avenue for preventing and treating rotaviral disease.

Materials and Methods

Mutagenesis of NSP2

The bacterial expression vector pQE60g8[16] encodes simian rotavirus SA11 NSP2 with a C-terminal His tag. To prepare a vector (pQEg8/Q3) encoding a mutant form of NSP2 with three amino acid substitutions in the basic grooves of the octamer (NSP2-Q3: K59Q/R60Q/R68Q), pQE60g8 was amplified by outward polymerase chain reaction (PCR) using Pfu Turbo DNA polymerase (Stratagene) and the primer pair, 5′-pAAG**C**AAC**A**GTATAATACTAATGATAATTCA**CA**AGGCAT-3′ and 5′-pAATTGAGGAGGTGGTGCTATTCC-3′. A vector (pQEg8/Q5) encoding an NSP2 mutant with five amino substitutions in the octamer grooves (NSP2-Q5: K37Q/K38Q/K59Q/R60Q/R68Q), was produced by PCR amplification using as template, pQE60g8/Q3, and the primers, 5′-pAAGTAGAC**C**AA**C**AGGACATGGATAAG-3′ and 5′ pTAGCTGTCAGCATAGCTTTAATAG-3′. A vector (pQEg8/Q6) encoding an NSP2 with six amino acid substitutions in the octamer grooves (NSP2-Q6: K37Q/K38Q/K58Q/K59Q/R60Q/R68Q) was produced by PCR amplification using as template, pQE60g8/Q5, and the primers, 5′-p**C**AGCAACAGTATAATACTAATGATAATTC-3′ and 5′-pAATTGAGGAGGTGGTGCTATTCC-3′. Bases in primers used to change codons in the NSP2 open reading frame (ORF) are denoted in bold. PCR products were gel-purified, self-ligated using T4 ligase, and transformed into *Escherichia coli* DH5α. Appropriate plasmids were identified by DNA sequencing, then transformed into *E. coli* M15 (pREP4). The preparation of the expression vector for NSP2 H225A was described.[18]

To produce pCI-based mammalian expression vectors encoding SA11 NSP2 (pCIg8), NSP2-Q3 (pCIg8/Q3), and NSP2-Q6 (pCIg8/Q6), the NSP2 ORFs in pQE60g8, pQE60g8/Q3 and pQE60g8/Q6, respectively, were amplified by PCR using the primer pair, 5′-GCTCTAGAATGGCTGAGCTAGCTTGCTTTTG-3′ and 5′-TATCTAGATTAAACGCCAACTTGAGAAAC-3′ (the XbaI site is underlined). A similar procedure was used to generate pCIg11, an expression vector encoding SA11 NSP5. The template used in the amplification reaction, pQE30g11,[47] contains a non-functional ORF for NSP6 due to a silent mutation that removes its initiation codon. The amplification reaction included the primer pair, 5′-GCTCTAGATGTCTCTCAGTATTGACGTGACG-3′ and 5′-TATCTAGATTACAAATCTTCAATCAATTGCATT-3′ (the XbaI site is underlined). Amplification products were gel-purified, digested with XbaI, ligated into the XbaI-site of the pCI vector (Promega), and transformed to *E. coli* DH5α. Appropriate pCI vectors were identified by DNA sequencing and were purified by centrifugation in CsCl/ethidium bromide.

Preparation of recombinant NSP2 and NSP5

Bacterial-expressed NSP2 and NSP5 were purified as described.[16,18,47] Briefly, NSP2 and NSP5 were expressed in *E. coli* M15(pREP4) using the vectors pQE60g8 and pQE30g11, respectively, and purified from bacterial lysates by Ni^{2+}-nitrilotriacetic acid affinity chromatography. NSP2 was dialyzed against low salt buffer (LSB: 2 mM Tris–HCl (pH 7.2), 0.5 mM EDTA, 0.5 mM dithiothreitol) supplemented with 50 mM NaCl. NSP5 was dialyzed briefly against 50 mM phosphate buffer (NaH_2PO_4) (pH 8.0), and 300 mM NaCl and then extensively in LSB supplemented

with 75 mM NaCl and 0.1% (v/v) Triton X-100. Protein concentrations were determined by Bradford assay using bovine serum albumin as the standard. Protein quality was assessed by SDS-12% (w/v) PAGE and staining with Coomassie blue. Recombinant NSP2 was purified to near homogeneity under conditions previously used to demonstrate the NTPase activity of the protein and to prepare protein for crystallography.[14,16] NSP5 contained trace (<1%) levels of DnaK.[47]

RNA synthesis *in vitro*

^{32}P-labeled gene *8*-specific RNAs were made with a MEGAshortscript high yield transcription kit (Ambion) following the instructions of the manufacturer, except that reaction mixtures (20 μl each) were modified to contain 7.5 mM each of ATP, CTP, and UTP, 1.87 mM GTP, and 50 μCi of [γ-^{32}P] or [α-^{32}P]GTP (6000 Ci/mmol) (American Radiolabeled Chemicals). The following annealed oligonucleotide pairs were included in reaction mixtures as templates for synthesis of 5′g8 and 5′g8m RNAs, respectively: 5′-GCCCTAATACGACTCACTATAGGCTTTTAAAGCGTCTCAGTC-3′ and 5′-GACTGAGACGCTTTTAAAAGCCTATAGTGAGTCGTATTAGGGC-3′, and 5′-GCCCTAATACGACTCACTATAGACTTTTAAAACATCTCAATC-3′ and 5′-GATTGAGATGTTTTAAAAGTCTATAGTGAGTCGTATTAGGGC-3′. (The T7 promoter sequence is underlined.) The 5′g8 RNA represents the first 21-nucleotides of the SA11 gene *8* (+)-strand RNA. The 5′ g8m RNA is the same as the g8 RNA, except that all but the G residue at the +1 position have been replaced with A residues.

The ^{32}P-labeled Luc200 RNA was made as described above except reaction mixtures contained 50 μCi of [α-^{32}P] UTP (800 Ci/mmol) (PerkinElmer), 1.87 mM UTP, and 7.5 mM each of ATP, CTP, and GTP. The template included in reaction mixtures was prepared by PCR amplification of a portion of the luciferase gene in the plasmid pGL2 (Promega) using the primer pair, 5′-GGCGGACAGGTATCCGG-3′ and 5′-GTTGCTCTCCAGCGGTTC-3′. A T7 promoter is provided by the amplified plasmid sequence. ^{32}P-labeled RNAs were gel-purified by electrophoresis on and elution from polyacrylamide gels containing 7 M urea.[16]

The [^{32}P]5′g8 capped RNA probe was prepared by incubating unlabeled 5′-g8 RNA with *S*-adenosyl methionine, [α-^{32}P]GTP (6000 Ci/mmol), and vaccinia-virus guanylyltransferase, according to the directions of the supplier (Ambion). After incubation for 1.5 h at 37 °C, the RNA was purified by phenol/chloroform extraction, followed by a size-exclusion chromatography (NucAway Spin Column; Ambion) to remove non-incorporated nucleotides. RNA concentrations were determined by UV absorbance at 260 nm.

RTPase assay

Unless indicated otherwise, reaction mixtures for RTPase assays contained 50 mM Tris–HCl (pH 7.5), 0.2 mM $MgCl_2$, 14 pmol of the [γ-^{32}P]5′g8 RNA, and 7 pmol of NSP2, in a final volume of 10 μl. After incubation for 1 h at 37 °C, reaction products were deproteinized by phenol/chloroform extraction and analyzed for P_i formation by TLC. Specifically, 3 μl aliquots of reaction mixtures were spotted onto polyethyleneimine-F cellulose (PEI-F) plates (EM Science), which were then air-dried. After predeveloping for 3 min in water, sheets were developed in 0.75 M potassium phosphate buffer (pH 3.4) to resolve $^{32}P_i$ and ^{32}P-labeled RNA. $^{32}P_i$ and ^{32}P-labeled RNA were detected by autoradiography and their intensities on the PEI sheets were quantified with a phosphorimager. P_i formation = intensity of (γ-$^{32}P_i$)/(intensity of (γ-$^{32}P_i$)+[γ-^{32}P] RNA).

To detect protein phosphorylation in RTPase assays, reaction mixtures were analyzed by SDS-12% PAGE and autoradiography. To assess the effects of the RTPase assay on the RNA component, one-half of reaction mixtures were analyzed by electrophoresis on 12% polyacrylamide gels containing 7 M urea. The gels were dried, and ^{32}P-labeled RNA detected by autoradiography.

RNase T1 treatment

RTPase assays were performed as above except reaction mixtures contained [α-^{32}P]g8-5′m RNA and 7 pmol of NSP2. After incubation for 1 h at 37 °C, some mixtures were adjusted to 5 mM EDTA, and incubated followed by a 20 min incubation at 37 °C in the presence of 500 U of RNase T1 (Ambion). After phenol/chloroform extraction, hydrolysis products were resolved by TLC in 1.2 M $LiCl_2$ and detected by autoradiography. Markers were made by incubating [α-^{32}P]GTP and RNase T1-treated [α-^{32}P]5′ g8m RNA with tobacco acid pyrophosphatase (TAP) (Epicentre) in 1× TAP reaction buffer (50 mM sodium acetate (pH 6.0), 1 mM EDTA, 0.1% (v/v) β-mercaptoethanol, 0. 01% (v/v) Triton X-100) for 15 min and 30 min at 37 °C, respectively. Partial hydrolysis with TAP was achieved by adding 1 mM GTP to the reaction mixture prior to incubation.

Decapping assays

Reaction mixtures contained 50 mM Tris–HCl (pH 7.5), 0.2 mM $MgCl_2$, 10 pmol of the [^{32}P]5′g8 capped RNA, and the indicated amount of *wtNSP2*, in a final volume of 20 μl. After incubation for 1 h at 37 °C, probe in reaction mixtures were analyzed by electrophoresis on 12% polyacrylamide gels containing 7 M urea and by autoradiography. Control reactions included incubating 10 pmol of [^{32}P]5′g8 capped RNA with 5 units of TAP for 1 h at 37 °C.

NTPase assay

NTP hydrolysis assays were performed as described.[16,18] Reaction mixtures contained 50 mM Tris–HCl (pH 7.5), 0.2 mM $MgCl_2$, 10 μCi [γ-^{32}P]ATP (3000 Ci/mmol) (PerkinElmer), and NSP2, and were incubated for 1 h at 37 °C. After deproteinization, aliquots (1 μl) of reaction mixtures were spotted onto PEI-F plates and the ATP, ADP and P_i components resolved by TLC in 1.2 M $LiCl_2$. Radioactive spots were detected by autoradiography and quantified with a phosphorimager. P_i formation = intensity of (γ-$^{32}P_i$)/(intensity of (γ-$^{32}P_i$)+ [γ-^{32}P]ATP).

RNA binding assays

Electrophoretic mobility shift assay (EMSA) was performed as described.[16] Reactions were performed in LSB containing the indicated amount of NSP2, 1 pmol of ^{32}P-labeled Luc200 RNA, and 100 mM NaCl, and were incubated for 30 min at room temperature (RT). Mixtures

were analyzed for RNA-protein complexes by electrophoresis on 6% non-denaturing polyacrylamide gels and autoradiography. The intensity of bands representing bound probe and free probe on dried gels were quantified with a phosphorimager. The quantity of protein–RNA complex represents the intensity of bound probe/intensity of bound probe + free probe.

Poly(U)-Sepharose RNA-binding assays were carried out in a manner similar to that described.[52] Briefly, 5 μg of NSP2 in 400 μl of LSB were incubated with 100 μl of a 50% slurry of poly(U)-Sepharose beads for 30 min at RT with gentle agitation. After washing twice with LSB, protein was eluted from the beads by sequential treatment with 100 μl volumes of LSB of increasing concentration of NaCl. The eluted fractions were analyzed for protein content by SDS-12% PAGE and silver staining with a Silver Quest kit (Invitrogen).

Molecular simulation of RNA

Similar to the methodology described,[18] the crystallographic data of rotavirus NSP2 (Protein Data Bank code 1L9V) was used for all calculations. The Autodock 3.02[48] program was used to perform a docking simulation of a 5-mer RNA molecule corresponding to the 5′ end of a rotavirus (+)-strand RNA (5′-pppGGCUU$_{OH}$) with NSP2. The size of the RNA selected for simulation was based on the limitation in the number of rotatable bonds imposed by the docking program. The Mg^{2+} was positioned in the cleft using distance restraint between the geometric center of the atoms OH of Tyr171 and OE2 of Glu153, followed by energy-minimization. This location is based on the position proposed for Mg^{2+} from the crystallographic data.[14] Representations of the NSP2 structure and 5-mer RNA were prepared using Insight II.[49] The hydrogen atoms of the protein and the RNA molecule were assigned by CHARMM (version 27).[50] Partial charges were assigned using the CHARMM27 Force Field. Atomic solvation parameters and fragmental volumes were assigned to the protein using the Addsol program. The grid maps were calculated using Autogrid and were centered on the ligand-binding site (NSP2 cleft). The volume chosen for the grid maps was $110 \times 100 \times 100$ points with a grid-point spacing of 0.375 Å. Autotors was used to define the rotatable bonds in the RNA fragment. In the docking simulation, the bonds between Pβ–O3B and Pγ–O3B at the 5′ end of RNA were restrained, emulating the conformation in which the triphosphate group is bound to the Mg^{2+}. The Lamarckian Genetic Algorithm was used for all docking calculations.

Among the ten best conformations, those with lowest free energy, one representative conformation with a reasonable distance between the oxygens of the γ-β phosphate groups at the 5′ end of RNA and the Mg^{2+} in the cleft was selected and used as starting point for an RNA binding simulation using molecular dynamics. The RNA–Mg^{2+}–NSP2 complex was then energy-minimized with harmonic restraint over all the backbone atoms and further analyzed after 1 nc of simulation (CHARMm).

NSP2 and NSP5 expression in mammalian cells

pCI vectors encoding NSP2 and/or NSP5 were transfected into MA104 cells grown to 60%–70% confluency on glass coverslips. Transfection mixtures (500 μl) consisted of OptiMEM I containing 4% (v/v) Lipofectamine 2000 (Invitrogen) and a total of 1.6 μg of DNA. Cells were processed for immunofluorescence at 40 h post-transfection.

Immunofluorescence microscopy

To detect expression of NSP2 and NSP5 by immunofluorescence assay (IFA), MA104 cells were fixed with 4% (v/v) paraformaldehyde, permeabilizing with 1% Triton X-100, and then incubated in the presence of NSP2-guinea pig polyclonal antisera (1:500)[16] and NSP5-mouse monoclonal antibody 158G37 (1:500).[51] Secondary antibodies conjugated to fluorescent dyes (Alexa Flour 488 goat anti-guinea pig and Alexa Flour 594 rabbit anti-mouse) were used at a dilution of 1:1000 to detect primary antibodies. Nuclei were stained with 4′, 6-diamidino-2-phenylindole (DAPI) (Pierce). Fluorescence was detected on a Leica TCS NT inverted confocal microscope and images were processed using Adobe PhotoShop CS.

Acknowledgements

We thank Mario Barro and Juraj Kabat for their advice and assistance on this project. This research was supported by the Intramural Research Program of the National Institutes of Allergy and Infectious Diseases, NIH.

References

1. Parashar, U. D., Hummelman, E. G., Bresee, J. S., Miller, M. A. & Glass, R. I. (2003). Global illness and deaths caused by rotavirus disease in children. *Emerg. Infect. Dis.* **9**, 565–572.
2. Prasad, B. V., Wang, G. J., Clerx, J. P. & Chiu, W. (1988). Three-dimensional structure of rotavirus. *J. Mol. Biol.* **199**, 269–275.
3. Estes, M. K. (2001). Rotavirus and their Replication. In *Fields Fundamental Virology* (D.M., K. & Howley, P. M., eds), pp. 1747–1785, Lippincott Williams and Wilkins Press, Philadelphia.
4. Cohen, J. (1977). Ribonucleic acid polymerase activity associated with purified calf rotavirus. *J. Gen. Virol.* **36**, 395–402.
5. Helmberger-Jones, M. & Patton, J. T. (1986). Characterization of subviral particles in cells infected with simian rotavirus SA11. *Virology*, **155**, 655–665.
6. Petrie, B. L., Graham, D. Y., Hanssen, H. & Estes, M. K. (1982). Localization of rotavirus antigens in infected cells by ultrastructural immunocytochemistry. *J. Gen. Virol.* **63**, 457–467.
7. Petrie, B. L., Greenberg, H. B., Graham, D. Y. & Estes, M. K. (1984). Ultrastructural localization of rotavirus antigens using colloidal gold. *Virus Res.* **1**, 133–152.
8. Fabbretti, E., Afrikanova, I., Vascotto, F. & Burrone, O. R. (1999). Two non-structural rotavirus proteins, NSP2 and NSP5, form viroplasm-like structures *in vivo*. *J. Gen. Virol.* **80**, 333–339.
9. Silvestri, L. S., Taraporewala, Z. F. & Patton, J. T. (2004). Rotavirus replication: plus-sense templates for double-stranded RNA synthesis are made in viroplasms. *J. Virol.* **78**, 7763–7774.

10. Campagna, M., Eichwald, C., Vascotto, F. & Burrone, O. R. (2005). RNA interference of rotavirus segment 11 mRNA reveals the essential role of NSP5 in the virus replicative cycle. *J. Gen. Virol.* **86**, 1481–1487.
11. Gallegos, C. O. & Patton, J. T. (1989). Characterization of rotavirus replication intermediates: a model for the assembly of single-shelled particles. *Virology*, **172**, 616–627.
12. Aponte, C., Poncet, D. & Cohen, J. (1996). Recovery and characterization of a replicase complex in rotavirus-infected cells by using a monoclonal antibody against NSP2. *J. Virol.* **70**, 985–991.
13. Kattoura, M. D., Chen, X. & Patton, J. T. (1994). The rotavirus RNA-binding protein NS35 (NSP2) forms 10S multimers and interacts with the viral RNA polymerase. *Virology*, **202**, 803–813.
14. Jayaram, H., Taraporewala, Z., Patton, J. T. & Prasad, B. V. (2002). Rotavirus protein involved in genome replication and packaging exhibits a HIT-like fold. *Nature*, **417**, 311–315.
15. Taraporewala, Z. F., Jiang, X., Vasquez-Del Carpio, R., Jayaram, H., Prasad, B. V. & Patton, J. T. (2006). Structure-function analysis of rotavirus NSP2 octamer by using a novel complementation system. *J. Virol.* **80**, 7984–7994.
16. Taraporewala, Z., Chen, D. & Patton, J. T. (1999). Multimers formed by the rotavirus nonstructural protein NSP2 bind to RNA and have nucleoside triphosphatase activity. *J. Virol.* **73**, 9934–9943.
17. Taraporewala, Z. F. & Patton, J. T. (2001). Identification and characterization of the helix-destabilizing activity of rotavirus nonstructural protein NSP2. *J. Virol.* **75**, 4519–4527.
18. Carpio, R. V., Gonzalez-Nilo, F. D., Jayaram, H., Spencer, E., Prasad, B. V., Patton, J. T. & Taraporewala, Z. F. (2004). Role of the histidine triad-like motif in nucleotide hydrolysis by the rotavirus RNA-packaging protein NSP2. *J. Biol. Chem.* **279**, 10624–10633.
19. Schuck, P., Taraporewala, Z., McPhie, P. & Patton, J. T. (2001). Rotavirus nonstructural protein NSP2 self-assembles into octamers that undergo ligand-induced conformational changes. *J. Biol. Chem.* **276**, 9679–9687.
20. Lima, C. D., Klein, M. G. & Hendrickson, W. A. (1997). Structure-based analysis of catalysis and substrate definition in the HIT protein family. *Science*, **278**, 286–290.
21. Kumar, M., Jayaram, H., Carpio, R., Jacobson, R., Patton, J. T. & Prasad, B. V. (2006). A novel viral NDP kinase with a cellular HIT fold.
22. Jiang, X., Jayaram, H., Ludtke, S., Estes, M. & Prasad, B. V. (2006). Cryo-EM structures of rotavirus NSP2-NSP5 and NSP2-RNA complexes: Implications for genome replication. *J. Virol.* In review.
23. Imai, M., Akatani, K., Ikegami, N. & Furuichi, Y. (1983). Capped and conserved terminal structures in human rotavirus genome double-stranded RNA segments. *J. Virol.* **47**, 125–136.
24. McCrae, M. A. & McCorquodale, J. G. (1983). Molecular biology of rotaviruses. V. Terminal structure of viral RNA species. *Virology*, **126**, 204–212.
25. Prasad, B. V., Rothnagel, R., Zeng, C. Q., Jakana, J., Lawton, J. A., Chiu, W. & Estes, M. K. (1996). Visualization of ordered genomic RNA and localization of transcriptional complexes in rotavirus. *Nature*, **382**, 471–473.
26. Lawton, J. A., Estes, M. K. & Prasad, B. V. (1997). Three-dimensional visualization of mRNA release from actively transcribing rotavirus particles. *Nature Struct. Biol.* **4**, 118–121.
27. Wang, Z. & Kiledjian, M. (2001). Functional link between the mammalian exosome and mRNA decapping. *Cell*, **107**, 751–762.
28. Gu, M., Fabrega, C., Liu, S.-W., Liu, H. & Lima, C. D. (2004). Insights into the structure, mechanism, and regulation of scavenger mRNA decapping activity. *Mol. Cell*, **14**, 67–80.
29. Spencer, E. & Garcia, B. I. (1984). Effect of *S*-adenosylmethionine on human rotavirus RNA synthesis. *J. Virol.* **52**, 188–197.
30. Chen, D., Luongo, C. L., Nibert, M. L. & Patton, J. T. (1999). Rotavirus open cores catalyze 5′-capping and methylation of exogenous RNA: evidence that VP3 is a methyltransferase. *Virology*, **265**, 120–130.
31. Liu, M., Mattion, N. M. & Estes, M. K. (1992). Rotavirus VP3 expressed in insect cells possesses guanylyltransferase activity. *Virology*, **188**, 77–84.
32. Chen, D. & Patton, J. T. (2000). *De novo* synthesis of minus strand RNA by the rotavirus RNA polymerase in a cell-free system involves a novel mechanism of initiation. *RNA*, **6**, 1455–1467.
33. Myette, J. R. & Niles, E. G. (1996). Characterization of the vaccinia virus RNA 5′-triphosphatase and nucleotide triphosphate phosphohydrolase activities. Demonstrate that both activities are carried out at the same active site. *J. Biol. Chem.* **271**, 11945–11952.
34. Gong, C. & Shuman, S. (2002). Chlorella virus RNA triphosphatase. Mutational analysis and mechanism of inhibition by tripolyphosphate. *J. Biol. Chem.* **277**, 15317–15324.
35. Lima, C. D., Wang, L. K. & Shuman, S. (1999). Structure and mechanism of yeast RNA triphosphatase: an essential component of the mRNA capping apparatus. *Cell*, **99**, 533–543.
36. Takagi, T., Moore, C. R., Diehn, F. & Buratowski, S. (1997). An RNA 5′-triphosphatase related to the protein tyrosine phosphatases. *Cell*, **89**, 867–873.
37. Changela, A., Ho, C. K., Martins, A., Shuman, S. & Mondragon, A. (2001). Structure and mechanism of the RNA triphosphatase component of mammalian mRNA capping enzyme. *EMBO J.* **20**, 2575–2586.
38. Changela, A., Martins, A., Shuman, S. & Mondragon, A. (2005). Crystal structure of baculovirus RNA triphosphatase complexed with phosphate. *J. Biol. Chem.* **280**, 17848–17856.
39. Benarroch, D., Selisko, B., Locatelli, G. A., Maga, G., Romette, J. L. & Canard, B. (2004). The RNA helicase, nucleotide 5′-triphosphatase, and RNA 5′-triphosphatase activities of Dengue virus protein NS3 are Mg^{2+}-dependent and require a functional Walker B motif in the helicase catalytic core. *Virology*, **328**, 208–218.
40. Bartelma, G. & Padmanabhan, R. (2002). Expression, purification, and characterization of the RNA 5′-triphosphatase activity of dengue virus type 2 nonstructural protein 3. *Virology*, **299**, 122–132.
41. Ivanov, K. A. & Ziebuhr, J. (2004). Human coronavirus 229E nonstructural protein 13: characterization of duplex-unwinding, nucleoside triphosphatase, and RNA 5′-triphosphatase activities. *J. Virol.* **78**, 7833–7838.
42. Vasiljeva, L., Merits, A., Auvinen, P. & Kaariainen, L. (2000). Identification of a novel function of the alphavirus capping apparatus. RNA 5′-triphosphatase activity of Nsp2. *J. Biol. Chem.* **275**, 17281–17287.
43. Taraporewala, Z. F. & Patton, J. T. (2004). Nonstructural proteins involved in genome packaging and replication of rotaviruses and other members of the Reoviridae. *Virus. Res.* **101**, 57–66.
44. Taraporewala, Z. F., Chen, D. & Patton, J. T. (2001). Multimers of the bluetongue virus nonstructural

protein, NS2, possess nucleotidyl phosphatase activity: similarities between NS2 and rotavirus NSP2. *Virology*, **280**, 221–231.
45. Gillian, A. L., Schmechel, S. C., Livney, J., Schiff, L. A. & Nibert, M. L. (2004). Reovirus protein sigmaNS binds in multiple copies to single-stranded RNA and shares properties with single-stranded DNA binding proteins. *J. Virol.* **74**, 5939–5948.
46. Kim, J., Parker, J. S., Murray, K. E. & Nibert, M. L. (2004). Nucleoside and RNA triphosphatase activities of orthoreovirus transcriptase cofactor mu2. *J. Biol. Chem.* **279**, 4394–4403.
47. Vende, P., Taraporewala, Z. F. & Patton, J. T. (2002). RNA-binding activity of the rotavirus phosphoprotein NSP5 includes affinity for double-stranded RNA. *J. Virol.* **76**, 5291–5299.
48. Morris, G. M., Goodsell, D. S., Halliday, R. S., Huey, R., Hart, W. E., Belew, R. K. & Olson, A. J. (1998). Automated docking using a Lamarckian genetic algorithm and an empirical binding free energy function. *J. Comp. Chem.* **19**, 1639–1662.
49. Accelrys (2006). *Insight II and Delphi user guide*, Accelrys, San Diego.
50. Brooks, B. R., Bruccoleri, R. E., Olafson, B. D., States, D. J., Swaminathan, S. & Karplus, M. (1983). CHARMM: a program for macromolecular energy, minimization, and dynamics calculations. *J. Comp. Chem.* **4**, 187–217.
51. Poncet, D., Lindenbaum, P., L'Haridon, R. & Cohen, J. (1997). *In vivo* and *in vitro* phosphorylation of rotavirus NSP5 correlates with its localization in viroplasms. *J. Virol.* **71**, 34–41.
52. Kattoura, M., Clapp, L. L. & Patton, J. T. (1992). The rotavirus nonstructural protein NS35 is a non-specific RNA-binding protein. *Virology*, **191**, 698–708.
53. Bisaillon, M. & Lemay, G. (1997). Characterization of the reovirus λ1 protein RNA 5′-triphosphatase activity. *J. Biol. Chem.* **272**, 29954–29957.
54. Bisaillon, M., Bergeron, J. & Lemay, G. (1997). Characterization of the nucleoside triphosphate phosphohydrolase and helicase activities of the reovirus λ1 protein. *J. Biol. Chem.* **272**, 18298–18303.

Edited by D. E. Draper

(Received 2 June 2006; received in revised form 13 July 2006; accepted 20 July 2006)
Available online 29 July 2006